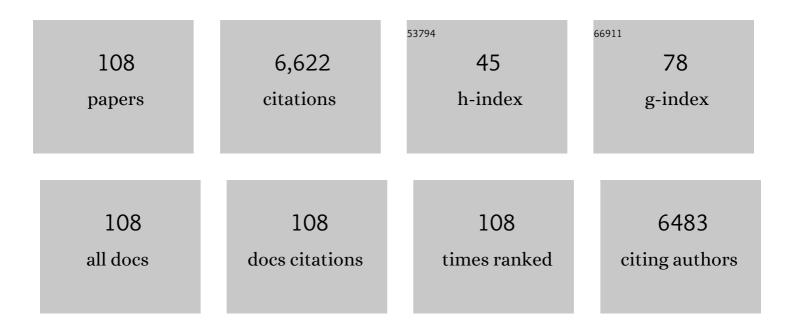


## List of Publications by Year in descending order

Source: https://exaly.com/author-pdf/1521989/publications.pdf Version: 2024-02-01



KAL TAO

#	Article	IF	CITATIONS
1	Fmoc-modified amino acids and short peptides: simple bio-inspired building blocks for the fabrication of functional materials. Chemical Society Reviews, 2016, 45, 3935-3953.	38.1	366
2	Self-assembling peptide semiconductors. Science, 2017, 358, .	12.6	357
3	Design of a porous cobalt sulfide nanosheet array on Ni foam from zeolitic imidazolate frameworks as an advanced electrode for supercapacitors. Nanoscale, 2018, 10, 2735-2741.	5.6	253
4	Shish-kebab type MnCo2O4@Co3O4 nanoneedle arrays derived from MnCo-LDH@ZIF-67 for high-performance supercapacitors and efficient oxygen evolution reaction. Chemical Engineering Journal, 2018, 354, 875-884.	12.7	205
5	A Zinc Cobalt Sulfide Nanosheet Array Derived from a 2D Bimetallic Metal–Organic Frameworks for Highâ€Performance Supercapacitors. Chemistry - A European Journal, 2018, 24, 12584-12591.	3.3	194
6	A metal–organic framework derived hierarchical nickel–cobalt sulfide nanosheet array on Ni foam with enhanced electrochemical performance for supercapacitors. Dalton Transactions, 2018, 47, 3496-3502.	3.3	188
7	Co3O4@CoNi-LDH core/shell nanosheet arrays for high-performance battery-type supercapacitors. Chemical Engineering Journal, 2018, 350, 551-558.	12.7	176
8	MOF-derived hierarchical double-shelled NiO/ZnO hollow spheres for high-performance supercapacitors. Dalton Transactions, 2016, 45, 13311-13316.	3.3	172
9	Enhanced photocatalytic performance of BiOBr/NH <sub>2</sub> -MIL-125(Ti) composite for dye degradation under visible light. Dalton Transactions, 2016, 45, 17521-17529.	3.3	171
10	MOF–derived hollow double–shelled NiO nanospheres for high–performance supercapacitors. Journal of Alloys and Compounds, 2018, 734, 1-8.	5.5	152
11	Photoactive properties of supramolecular assembled short peptides. Chemical Society Reviews, 2019, 48, 4387-4400.	38.1	150
12	Non-proteinaceous hydrolase comprised of a phenylalanine metallo-supramolecular amyloid-like structure. Nature Catalysis, 2019, 2, 977-985.	34.4	142
13	Formation of bimetallic metal–organic framework nanosheets and their derived porous nickel–cobalt sulfides for supercapacitors. Dalton Transactions, 2018, 47, 5639-5645.	3.3	127
14	Quantum confined peptide assemblies with tunable visible to near-infrared spectral range. Nature Communications, 2018, 9, 3217.	12.8	122
15	Ultrathin Ni-MOF nanosheet arrays grown on polyaniline decorated Ni foam as an advanced electrode for asymmetric supercapacitors with high energy density. Dalton Transactions, 2019, 48, 4119-4123.	3.3	122
16	Metal-Ion Modulated Structural Transformation of Amyloid-Like Dipeptide Supramolecular Self-Assembly. ACS Nano, 2019, 13, 7300-7309.	14.6	121
17	High performance ZIF-8 molecular sieve membrane on hollow ceramic fiber via crystallizing-rubbing seed deposition. Chemical Engineering Journal, 2013, 220, 1-5.	12.7	118
18	Construction of 2D ZIF-derived hierarchical and hollow NiCo-LDH "nanosheet-on-nanosheet―arrays on reduced graphene oxide/Ni foam for boosted electrochemical energy storage. Journal of Alloys and Compounds, 2021, 850, 156864.	5.5	109

#	Article	IF	CITATIONS
19	ZIF-Derived Porous CoNi <sub>2</sub> S <sub>4</sub> on Intercrosslinked Polypyrrole Tubes for High-Performance Asymmetric Supercapacitors. ACS Applied Energy Materials, 2021, 4, 4199-4207.	5.1	108
20	Ultrathin nanosheet-assembled hollow microplate CoMoO4 array derived from metal-organic framework for supercapacitor with ultrahigh areal capacitance. Journal of Power Sources, 2019, 430, 51-59.	7.8	98
21	In Situ Growth of Metal–Organic Framework on BiOBr 2D Material with Excellent Photocatalytic Activity for Dye Degradation. Crystal Growth and Design, 2017, 17, 2309-2313.	3.0	97
22	Recent advances in metal–organic framework-based electrode materials for supercapacitors. Dalton Transactions, 2021, 50, 11701-11710.	3.3	93
23	Facile Carbonization of Microporous Organic Polymers into Hierarchically Porous Carbons Targeted for Effective CO <sub>2</sub> Uptake at Low Pressures. ACS Applied Materials & Interfaces, 2016, 8, 18383-18392.	8.0	90
24	A hierarchical NiO/NiMn-layered double hydroxide nanosheet array on Ni foam for high performance supercapacitors. Dalton Transactions, 2017, 46, 7388-7391.	3.3	88
25	Hierarchical Two-Dimensional Conductive Metal–Organic Framework/Layered Double Hydroxide Nanoarray for a High-Performance Supercapacitor. Inorganic Chemistry, 2018, 57, 6202-6205.	4.0	86
26	Construction of Ni-Co-Mn layered double hydroxide nanoflakes assembled hollow nanocages from bimetallic imidazolate frameworks for supercapacitors. Materials Research Bulletin, 2018, 106, 243-249.	5.2	83
27	Bioinspired Stable and Photoluminescent Assemblies for Power Generation. Advanced Materials, 2019, 31, e1807481.	21.0	82
28	Solvent-Controlled Morphology of Amino-Functionalized Bimetal Metal–Organic Frameworks for Asymmetric Supercapacitors. Inorganic Chemistry, 2020, 59, 11385-11395.	4.0	82
29	Metal–Organic Framework Templated 3D Hierarchical ZnCo <sub>2</sub> O <sub>4</sub> @Ni(OH) <sub>2</sub> Core–Shell Nanosheet Arrays for Highâ€Performance Supercapacitors. Chemistry - A European Journal, 2018, 24, 18106-18114.	3.3	79
30	Inlaying ZIF-derived Co3S4 hollow nanocages on intertwined polypyrrole tubes conductive networks for high-performance supercapacitors. Electrochimica Acta, 2020, 341, 136042.	5.2	73
31	Self-supported metal–organic framework-based nanostructures as binder-free electrodes for supercapacitors. Nanoscale, 2022, 14, 2155-2166.	5.6	73
32	Construction of NiCo <sub>2</sub> O <sub>4</sub> nanosheet-decorated leaf-like Co <sub>3</sub> O <sub>4</sub> nanoarrays from metal–organic framework for high-performance hybrid supercapacitors. Dalton Transactions, 2019, 48, 14156-14163.	3.3	72
33	Core–shell assembly of carbon nanofibers and a 2D conductive metal–organic framework as a flexible free-standing membrane for high-performance supercapacitors. Inorganic Chemistry Frontiers, 2019, 6, 1824-1830.	6.0	70
34	Stable and optoelectronic dipeptide assemblies for power harvesting. Materials Today, 2019, 30, 10-16.	14.2	62
35	A hollow ceramic fiber supported ZIF-8 membrane with enhanced gas separation performance prepared by hot dip-coating seeding. Journal of Materials Chemistry A, 2013, 1, 13046.	10.3	60
36	Diphenylalanine-Derivative Peptide Assemblies with Increased Aromaticity Exhibit Metal-like Rigidity and High Piezoelectricity. ACS Nano, 2020, 14, 7025-7037.	14.6	59

#	Article	IF	CITATIONS
37	Zeolitic imidazolate framework-derived Co <sub>3</sub> S <sub>4</sub> @Co(OH) <sub>2</sub> nanoarrays as self-supported electrodes for asymmetric supercapacitors. Inorganic Chemistry Frontiers, 2019, 6, 1398-1404.	6.0	57
38	Controlled synthesis of Pd–NiO@SiO <sub>2</sub> mesoporous core–shell nanoparticles and their enhanced catalytic performance for p-chloronitrobenzene hydrogenation with H <sub>2</sub> . Catalysis Science and Technology, 2015, 5, 405-414.	4.1	56
39	In situ growth of ZIF-8 nanocrystals on layered double hydroxide nanosheets for enhanced CO <sub>2</sub> capture. Dalton Transactions, 2016, 45, 12632-12635.	3.3	55
40	Metalâ€Organic Frameworksâ€Derived Porous In <sub>2</sub> O <sub>3</sub> Hollow Nanorod for Highâ€Performance Ethanol Gas Sensor. ChemistrySelect, 2017, 2, 10918-10925.	1.5	55
41	Influence of Ovalbumin on CaCO <sub>3</sub> Precipitation during <i>in Vitro</i> Biomineralization. Journal of Physical Chemistry B, 2010, 114, 5301-5308.	2.6	50
42	Enhanced catalytic performance of molybdenum-doped mesoporous SBA-15 for metathesis of 1-butene and ethene to propene. Catalysis Science and Technology, 2014, 4, 4010-4019.	4.1	50
43	Hierarchical core–shell SiO <sub>2</sub> @PDA@BiOBr microspheres with enhanced visible-light-driven photocatalytic performance. Dalton Transactions, 2017, 46, 11451-11458.	3.3	49
44	High-Efficiency Fluorescence through Bioinspired Supramolecular Self-Assembly. ACS Nano, 2020, 14, 2798-2807.	14.6	49
45	Co <sub>3</sub> S <sub>4</sub> Nanoplate Arrays Decorated with Oxygen-Deficient CeO <sub>2</sub> Nanoparticles for Supercapacitor Applications. ACS Applied Nano Materials, 2021, 4, 3033-3043.	5.0	49
46	Design of Mo-doped cobalt sulfide hollow nanocages from zeolitic imidazolate frameworks as advanced electrodes for supercapacitors. Inorganic Chemistry Frontiers, 2019, 6, 2178-2184.	6.0	48
47	Short peptide-directed synthesis of one-dimensional platinum nanostructures with controllable morphologies. Scientific Reports, 2013, 3, 2565.	3.3	45
48	Hierarchical core–shell 2D MOF nanosheet hybrid arrays for high-performance hybrid supercapacitors. Dalton Transactions, 2021, 50, 8179-8188.	3.3	44
49	Piezoelectric Peptide and Metabolite Materials. Research, 2019, 2019, 9025939.	5.7	44
50	Engineering coordination polymer-derived one-dimensional porous S-doped Co <sub>3</sub> O <sub>4</sub> nanorods with rich oxygen vacancies as high-performance electrode materials for hybrid supercapacitors. Dalton Transactions, 2020, 49, 10421-10430.	3.3	42
51	MOF-derived Bi <sub>2</sub> O <sub>3</sub> @C microrods as negative electrodes for advanced asymmetric supercapacitors. RSC Advances, 2020, 10, 14107-14112.	3.6	41
52	Development of platinum-based bimodal pore catalyst for CO2 reforming of CH4. Catalysis Today, 2010, 153, 150-155.	4.4	40
53	Fabrication of 2D/2D nanosheet heterostructures of ZIF-derived Co <sub>3</sub> S <sub>4</sub> and g-C <sub>3</sub> N <sub>4</sub> for asymmetric supercapacitors with superior cycling stability. Dalton Transactions, 2020, 49, 14017-14029.	3.3	40
54	Accelerated charge transfer in water-layered peptide assemblies. Energy and Environmental Science, 2020. 13. 96-101.	30.8	39

#	Article	IF	CITATIONS
55	Tanghulu-like NiO microcubes on Co3O4 nanowires arrays anchored on Ni foam with improved electrochemical performances for supercapacitors. Journal of Alloys and Compounds, 2018, 748, 496-503.	5.5	38
56	Conductive 2D Metalâ€Organic Frameworks Decorated on Layered Double Hydroxides Nanoflower Surface for Highâ€Performance Supercapacitor. ChemistrySelect, 2018, 3, 13596-13602.	1.5	35
57	Heterostructure of metal–organic framework-derived straw-bundle-like CeO2 decorated with (Ni,) Tj ETQq1 1 (	).784314 ı 6.1	rg₿Ţ /Overl⊙
58	Chemical and spatial promotional effects of bimodal pore catalysts for methane dry reforming. Chemical Engineering Journal, 2011, 170, 258-263.	12.7	33
59	Stringing metal–organic framework-derived hollow Co3S4 nanopolyhedra on V2O5 nanowires for high-performance supercapacitors. Applied Surface Science, 2022, 600, 154076.	6.1	33
60	Multiporous Supramolecular Microspheres for Artificial Photosynthesis. Chemistry of Materials, 2017, 29, 4454-4460.	6.7	32
61	Controllable In Situ Transformation of Layered Double Hydroxides into Ultrathin Metal–Organic Framework Nanosheet Arrays for Energy Storage. Inorganic Chemistry, 2022, 61, 3832-3842.	4.0	32
62	Microwave-assisted synthesis of pillared Ni-based metal–organic framework and its derived hierarchical NiO nanoparticles for supercapacitors. Journal of Materials Science: Materials in Electronics, 2018, 29, 14697-14704.	2.2	31
63	Cobalt-Borate Nanoarray: An Efficient and Durable Electrocatalyst for Water Oxidation under Benign Conditions. ACS Applied Materials & Interfaces, 2017, 9, 15383-15387.	8.0	30
64	Core–shell assembly of Co <sub>3</sub> O <sub>4</sub> @NiO-ZnO nanoarrays as battery-type electrodes for high-performance supercapatteries. Inorganic Chemistry Frontiers, 2019, 6, 2481-2487.	6.0	30
65	Metal-organic frameworks derived porous carbon coated SiO composite as superior anode material for lithium ion batteries. Journal of Alloys and Compounds, 2018, 765, 512-519.	5.5	29
66	NiCo <sub>2</sub> S <sub>4</sub> @Ni <sub>3</sub> S <sub>2</sub> hybrid nanoarray on Ni foam for high-performance supercapacitors. New Journal of Chemistry, 2019, 43, 7344-7349.	2.8	29
67	Construction of S-doped ZnCo2O4 microspindles with enhanced electrochemical performance for supercapacitors. Vacuum, 2020, 181, 109740.	3.5	29
68	Construction of Hierarchical 2D PANI/Ni <sub>3</sub> S <sub>2</sub> Nanosheet Arrays on Ni Foam for Highâ€Performance Asymmetric Supercapacitors. Batteries and Supercaps, 2020, 3, 370-375.	4.7	29
69	Boosting the energy storage performance of MOF-derived Co <sub>3</sub> S <sub>4</sub> nanoarrays <i>via</i> sulfur vacancy and surface engineering. Chemical Communications, 2022, 58, 6243-6246.	4.1	29
70	MOF-derived hierarchical core–shell hollow Co <sub>3</sub> S <sub>4</sub> @NiCo <sub>2</sub> O <sub>4</sub> nanosheet arrays for asymmetric supercapacitors. Dalton Transactions, 2022, 51, 4406-4413.	3.3	27
71	Optical property modulation of Fmoc group by pH-dependent self-assembly. RSC Advances, 2015, 5, 73914-73918.	3.6	25
72	Metal-Organosulfide Coordination Polymer Nanosheet Array as a Battery-Type Electrode for an Asymmetric Supercapacitor. Inorganic Chemistry, 2020, 59, 7360-7369.	4.0	25

#	Article	IF	CITATIONS
73	Sol–gel auto-combustion synthesis of Ni–CexZr1â^'xO2 catalysts for carbon dioxide reforming of methane. RSC Advances, 2013, 3, 22285.	3.6	24
74	Enhanced catalytic performance for metathesis reactions over ordered tungsten and aluminum co-doped mesoporous KIT-6 catalysts. New Journal of Chemistry, 2015, 39, 7971-7978.	2.8	24
75	Mechanically rigid supramolecular assemblies formed from an Fmoc-guanine conjugated peptide nucleic acid. Nature Communications, 2019, 10, 5256.	12.8	24
76	Design of trimetallic sulfide hollow nanocages from metal–organic frameworks as electrode materials for supercapacitors. Dalton Transactions, 2021, 50, 15260-15266.	3.3	24
77	Enhanced Capacitance Performance by Coupling 2D Conductive Metal–Organic Frameworks and Conducting Polymers for Hybrid Supercapacitors. ACS Applied Energy Materials, 2021, 4, 9534-9541.	5.1	24
78	Studying structure and dynamics of self-assembled peptide nanostructures using fluorescence and super resolution microscopy. Chemical Communications, 2017, 53, 7294-7297.	4.1	23
79	Controlled Preparation of Hollow and Porous Co <sub>9</sub> S <sub>8</sub> Microplate Arrays for High-Performance Hybrid Supercapacitors. Inorganic Chemistry, 2020, 59, 11174-11183.	4.0	23
80	Precisely designing bimodal catalyst structure to trap cobalt nanoparticles inside mesopores and its application in Fischer-Tropsch synthesis. Chemical Engineering Journal, 2016, 306, 784-790.	12.7	22
81	MOF-assisted construction of a Co <sub>9</sub> S <sub>8</sub> @Ni <sub>3</sub> S <sub>2</sub> /ZnS microplate array with ultrahigh areal specific capacity for advanced supercapattery. Dalton Transactions, 2020, 49, 10535-10544.	3.3	22
82	Tandem catalytic conversion of 1-butene and ethene to propene over combined mesoporous W-FDU-12 and MgO catalysts. RSC Advances, 2015, 5, 23981-23989.	3.6	19
83	Bi <sub>2</sub> S <sub>3</sub> nanorod-stacked hollow microtubes self-assembled from bismuth-based metal–organic frameworks as advanced negative electrodes for hybrid supercapacitors. Dalton Transactions, 2019, 48, 9057-9061.	3.3	19
84	Bioinspired Supramolecular Packing Enables High Thermoâ€Sustainability. Angewandte Chemie - International Edition, 2020, 59, 19037-19041.	13.8	18
85	Interfacial adsorption of lipopeptidesurfactants at the silica/water interface studied by neutron reflection. Soft Matter, 2011, 7, 1777-1788.	2.7	17
86	Design of Controllable Bio-Inspired Chiroptic Self-Assemblies. Biomacromolecules, 2016, 17, 2937-2945.	5.4	17
87	Hollow and Hierarchical Cobalt–Metal Organic Framework@CoCr <sub>2</sub> O <sub>4</sub> Microplate Array as a Batteryâ€Type Electrode for Highâ€Performance Hybrid Supercapacitors. ChemElectroChem, 2020, 7, 437-444.	3.4	17
88	Controllable Transformation of Metal–Organic Framework Nanosheets into Oxygen Vacancy Ni <sub><i>x</i></sub> Co <sub>3–<i>x</i></sub> O <sub>4</sub> Arrays for Ultrahigh-Capacitance Supercapacitors with Long Lifespan. Inorganic Chemistry, 2022, 61, 4283-4291.	4.0	17
89	Zeolitic imidazolate framework derived ZnCo <sub>2</sub> O <sub>4</sub> hollow tubular nanofibers for long-life supercapacitors. RSC Advances, 2020, 10, 13922-13928.	3.6	16
90	High-performance supercapacitors of Cu-based porous coordination polymer nanowires and the derived porous CuO nanotubes. Dalton Transactions, 2017, 46, 16821-16827.	3.3	15

#	Article	IF	CITATIONS
91	CO2 hydrogenation to methanol over Cu/ZnO catalysts synthesized via a facile solid-phase grinding process using oxalic acid. Korean Journal of Chemical Engineering, 2018, 35, 110-117.	2.7	15
92	Self-Assembly of Cyclic Dipeptides: Platforms for Functional Materials. Protein and Peptide Letters, 2020, 27, 688-697.	0.9	15
93	Metathesis of 1-butene and ethene to propene over mesoporous W-KIT-6 catalysts: the influence of Si/W ratio. Journal of Porous Materials, 2015, 22, 613-620.	2.6	13
94	Metal–Organic Framework-Derived Bi <sub>2</sub> O <sub>3</sub> /C and NiCo <sub>2</sub> S <sub>4</sub> Hollow Nanofibers for Asymmetric Supercapacitors. ACS Applied Nano Materials, 2021, 4, 11895-11906.	5.0	13
95	Mesoporous Ni2CoS4 electrode materials derived from coordination polymer bricks for high-performance supercapacitor. Journal of Solid State Chemistry, 2019, 271, 239-245.	2.9	11
96	Enhanced Hydrogen Production from Steam Reforming of Vegetable Oil over Bimodal ZrO <sub>2</sub> â€&iO <sub>2</sub> Supported Ni Catalyst. ChemistrySelect, 2017, 2, 527-532.	1.5	10
97	A Self-Bleaching Electrochromic Mirror Based on Metal Organic Frameworks. Materials, 2021, 14, 2771.	2.9	10
98	Transformation of Au3M/SiO2 (MÂ=ÂNi, Co, Fe) into Au–MO x /SiO2 Catalysts for the Reduction of p-Nitrophenol. Catalysis Letters, 2014, 144, 1001-1008.	2.6	9
99	Entropy Method for Structural Health Monitoring Based on Statistical Cause and Effect Analysis of Acoustic Emission and Vibration Signals. IEEE Access, 2019, 7, 172515-172525.	4.2	9
100	Entropic Phase Transitions with Stable Twisted Intermediates of Bioâ€Inspired Selfâ€Assembly. Chemistry - A European Journal, 2016, 22, 15237-15241.	3.3	8
101	Preparation of Polydopamine-Modified 3D Interconnected Macroporous Silica for Laccase Immobilization. Macromolecular Research, 2018, 26, 616-622.	2.4	7
102	Bioinspired Suprahelical Frameworks as Scaffolds for Artificial Photosynthesis. ACS Applied Materials & Interfaces, 2020, 12, 45192-45201.	8.0	7
103	An anthropomorphic fuzzy model for the time-spatial assessment of sandstone seepage damage. Automation in Construction, 2020, 109, 102989.	9.8	6
104	Modulating vectored non-covalent interactions for layered assembly with engineerable properties. Bio-Design and Manufacturing, 2022, 5, 529-539.	7.7	6
105	Controllable Phase Separation by Boc-Modified Lipophilic Acid as a Multifunctional Extractant. Scientific Reports, 2015, 5, 17509.	3.3	4
106	Preparation of Hierarchical Porous Sâ€1/silica Monoliths by Steaming Crystallization. ChemistrySelect, 2019, 4, 3741-3744.	1.5	4
107	EDTA-mimicking amino acid–metal ion coordination for multifunctional packings. Journal of Materials Chemistry A, 2021, 9, 20385-20394.	10.3	4
108	Bioinspired Supramolecular Packing Enables High Thermo‧ustainability. Angewandte Chemie, 2020, 132, 19199-19203.	2.0	2